



# An inventory of interactors of the human HSP60/HSP10 chaperonin in the mitochondrial matrix space

Anne Sigaard Bie<sup>1</sup> · Cagla Cömert<sup>1</sup> · Roman Körner<sup>2</sup> · Thomas J. Corydon<sup>3,4</sup> · Johan Palmfeldt<sup>1</sup> · Mark S. Hipp<sup>2,5,6</sup> · F. Ulrich Hartl<sup>2</sup> · Peter Bross<sup>1</sup>

Received: 9 December 2019 / Revised: 14 January 2020 / Accepted: 10 February 2020 / Published online: 14 February 2020  
© Cell Stress Society International 2020

## Abstract

The HSP60/HSP10 chaperonin assists folding of proteins in the mitochondrial matrix space by enclosing them in its central cavity. The chaperonin forms part of the mitochondrial protein quality control system. It is essential for cellular survival and mutations in its subunits are associated with rare neurological disorders. Here we present the first survey of interactors of the human mitochondrial HSP60/HSP10 chaperonin. Using a protocol involving metabolic labeling of HEK293 cells, cross-linking, and immunoprecipitation of HSP60, we identified 323 interacting proteins. As expected, the vast majority of these proteins are localized to the mitochondrial matrix space. We find that approximately half of the proteins annotated as mitochondrial matrix proteins interact with the HSP60/HSP10 chaperonin. They cover a broad spectrum of functions and metabolic pathways including the mitochondrial protein synthesis apparatus, the respiratory chain, and mitochondrial protein quality control. Many of the genes encoding HSP60 interactors are annotated as disease genes. There is a correlation between relative cellular abundance and relative abundance in the HSP60 immunoprecipitates. Nineteen abundant matrix proteins occupy more than 60% of the HSP60/HSP10 chaperonin capacity. The reported inventory of interactors can form the basis for interrogating which proteins are especially dependent on the chaperonin.

**Keywords** HSP60 · HSP10 · Molecular chaperone · Chaperonin · Mitochondrial protein quality control · Protein folding

**Electronic supplementary material** The online version of this article (<https://doi.org/10.1007/s12192-020-01080-6>) contains supplementary material, which is available to authorized users.

✉ Peter Bross  
[peter.bross@clin.au.dk](mailto:peter.bross@clin.au.dk)

- <sup>1</sup> Research Unit for Molecular Medicine, Department of Clinical Medicine, Aarhus University and Aarhus University Hospital, Palle Juul-Jensens Boulevard 99, 8200 Aarhus N, Denmark
- <sup>2</sup> Department of Cellular Biochemistry, Max Planck Institute of Biochemistry, Am Klopferspitz 18, D-82152 Martinsried, Germany
- <sup>3</sup> Department of Biomedicine, Aarhus University, Hoegh-Guldbergsgade 10, 8000 Aarhus C, Denmark
- <sup>4</sup> Department of Ophthalmology, Aarhus University Hospital, Palle Juul-Jensens Boulevard 99, 8200 Aarhus N, Denmark
- <sup>5</sup> Department of Biomedical Sciences of Cells and Systems, University Medical Center Groningen, University of Groningen, Antonius Deusinglaan 1, 9713 AV Groningen, The Netherlands
- <sup>6</sup> School of Medicine and Health Sciences, Carl von Ossietzky University Oldenburg, 26111 Oldenburg, Germany

## Introduction

The HSP60/HSP10 chaperonin, a molecular chaperone in the mitochondrial matrix space, is essential for survival of eukaryotic cells (Christensen et al. 2010). Molecular chaperones recognize and intermittently bind folding intermediates and promote their folding to the native state (Hartl and Hayer-Hartl 2009). Together with proteases and accessory factors they take care of protein quality control and maintain protein homeostasis, in short proteostasis, an essential triage process that on one side facilitates and safeguards protein folding and on the other removes misfolded proteins that may otherwise aggregate and disturb cellular processes (Gottesman et al. 1997; Hipp et al. 2019). Protein misfolding is a widely observed feature in diseases and associated with numerous degenerative disorders. These include both toxic gain-of-function diseases like Huntington's, Alzheimer's, and Parkinson's disease, where misfolded proteins aggregate, but also many inherited deficiencies that typically result in loss-of-function, when misfolded mutant proteins are proteolytically degraded

(Gregersen et al. 2006; Kim et al. 2013). Pathological protein misfolding can also be caused by environmental stress or by mutations in genes encoding protein quality control components, like chaperones and proteases. Remarkably, a whole series of rare human disorders affecting components of mitochondrial protein quality control chaperones and proteases have been described (Bie et al. 2016; Casari et al. 1998; Di Bella et al. 2010; Dikoglu et al. 2015; Hansen et al. 2002; Jenkinson et al. 2013; Royer-Bertrand et al. 2015; Saisawat et al. 2014). In particular, a number of rare phenotypically distinct human neurological diseases are associated with mutations in the *HSPD1* and *HSPE1* genes encoding human HSP60 and HSP10, respectively (Bie et al. 2016; Bross et al. 2008; Hansen et al. 2002; Magen et al. 2008). The HSP60 and HSP10 proteins are expressed at high levels in all tissues. It is therefore unclear why inherited deficiencies of this chaperonin primarily affect neuronal tissues and apparently have no noticeable impact on other tissues, such as the muscle cells of heart and skeletal muscle, both of which are highly dependent on mitochondria as energy source. Secondary HSP60/HSP10 deficiency has been implicated as a disease mechanism in Parkinson's disease (Szegő et al. 2019). Here, cytosolic trapping of HSP10 in synuclein aggregates may contribute to HSP60/HSP10 chaperonin deficiency, resulting in mitochondrial dysfunction observed in Parkinson's disease. Despite many years of research on the HSP60/HSP10 chaperonin, the spectrum of mitochondrial proteins using this chaperonin is still poorly defined.

The chaperone function of the mitochondrial HSP60 was first recognized in experiments with a temperature-sensitive mutant of yeast Hsp60 that resulted in failure to assemble mitochondrial ornithine transcarbamylase (OTC) and the  $\beta$ -subunit of F1-ATPase (F1 $\beta$ ) (Cheng et al. 1989). The primary role of Hsp60 in protein folding, rather than assembly, was demonstrated in experiments with the Hsp60 of the fungus *N. crassa* (Ostermann et al. 1989), and Hsp10 was characterized as an essential component of the mitochondrial Hsp60/Hsp10 system in yeast (Hohfeld and Hartl 1994). HSP60 and HSP10 and their orthologs in bacteria and plant chloroplasts are highly conserved between species (Bross 2015) and inactivating mutations in the *E. coli* (Fayet et al. 1989), yeast (Cheng et al. 1989), fly (Perezgasga et al. 1999), and mouse (Christensen et al. 2010) orthologs are lethal. In analogy to the prototype bacterial chaperonin GroEL/GroES (Hayer-Hartl et al. 2016), mitochondrial HSP60 assembles into double-rings forming a barrel structure with an inner cavity that can be closed by lids formed by HSP10 rings (Nisemblat et al. 2015). This architecture allows cycles of binding, encapsulation, folding, and release of proteins. These cycles involve conformational changes orchestrated by ATP binding and hydrolysis, allosteric communication between the HSP60 rings, and closing and opening of the cavity by the HSP10 lid (Levy-Rimler et al. 2002; Levy-Rimler et al. 2001).

Research on the GroEL/GroES chaperonin from *E. coli* has indicated that approximately 250–300 proteins out of the estimated 2500 cytoplasmic polypeptides of *E. coli* interact with the GroEL/GroES chaperonin (Houry et al. 1999). Subsequent investigations identified approximately 85 proteins that were suggested to be obligately dependent on the GroEL/GroES chaperonin for folding to the native state (Kerner et al. 2005). For approximately 60% of these proteins, GroEL dependence was confirmed (Fujiwara et al. 2010). Extrapolated to the mitochondrial matrix, which contains approximately 500 proteins (Rhee et al. 2013), this would mean that around 50 proteins interact with the HSP60/HSP10 chaperonin and 15–20 proteins would be obligately dependent. So far only a handful of mitochondrial matrix proteins have been reported to interact with the mammalian HSP60/HSP10 chaperonin in a manner modulating their folding. Examples are the fatty acid oxidation enzyme medium-chain acyl-CoA dehydrogenase (MCAD) (Saijo et al. 1994), the oxidative stress defense protein manganese superoxide dismutase (SOD2) (Magnoni et al. 2014), and the UQCRC1 subunit of respiratory chain complex III (Magnoni et al. 2013).

The present study is the first systematic survey of proteins interacting with the human HSP60/HSP10 complex. We show in HEK293 cells that the HSP60/HSP10 chaperonin interacts with a surprisingly large fraction of mitochondrial matrix proteins, covering a wide range of mitochondrial functions and pathways. The present study establishes an inventory of matrix proteins that interact with the HSP60/HSP10 chaperonin.

## Materials and methods

### Cell culturing, crosslinking, and IP

HEK293 cells were grown in Dulbecco's modified Eagle's medium (DMEM) containing 10% dialyzed fetal calf serum (PAA Laboratories), 50 units/ml penicillin, and 50  $\mu$ g/ml streptomycin. SILAC labeling of the HEK293 cells was performed as described previously (Ong and Mann 2006). Unlabeled and labeled arginine and lysine were added as follows: SILAC light: L-arginine (R0) and L-lysine (K0) (Sigma); SILAC medium: L-[U- $^{13}$ C $_6$ ,  $^{14}$ N $_4$ ]arginine (R6) and L-[ $^2$ H $_4$ ]lysine (K4); and SILAC heavy: L-[U- $^{13}$ C $_6$ ,  $^{15}$ N $_4$ ]arginine (R10) and L-[U- $^{13}$ C $_6$ ,  $^{15}$ N $_2$ ]lysine (K8) (all from Cambridge Isotope Laboratories). Cells were grown at 37 °C in the respective medium in a humidified incubator with 5% CO $_2$  atmosphere.

For heat-shock, cells were treated for 3 h at 43 °C followed by 12 h recovery at 37 °C. Before harvesting at approximately 90% confluency, cells were washed in PBS and incubated for 30 min with 5 mM cross-linker dithiobis (succinimidyl propionate) (DSP, Thermo Scientific, cat. no. 22585) in PBS. Crosslinking was quenched by addition of 50 mM Tris-HCl

pH 7.5. Cells were harvested using a cell scraper, counted, pelleted by centrifugation and lysed by three freeze/thaw cycles in a buffer containing 50 mM Tris-HCl pH 7.5, 50 mM NaCl, 5 mM EDTA, and supplemented with hexokinase to deplete ATP and protease inhibitors (complete protease inhibitor cocktail, EDTA-free (Sigma, cat. no. C2978)).

Co-immunoprecipitation was performed using Dynabeads M-270 epoxy (Invitrogen, cat. no. 143.01) covalently coupled to anti-HSP60 (Abcam cat. no. ab110312) or anti-GFP antibody (Abcam cat. no. ab3277) according to manufacturer's instructions with the following modification: samples were eluted from beads by boiling at 95 °C in 1x SDS sample buffer (60 mM Tris-HCl pH 6.8, 5% (v/v) glycerol, 1.66% (w/v) SDS, 0.1 M DTT).

### Western blotting

Cells were heat-shocked as described above. Prior to harvesting, cell density and morphology were recorded by imaging with a light microscope ( $\times 10$  magnification). Cells were harvested using a cell scraper and lysed in CelLytic M (Sigma, cat. no. C2978) lysis buffer supplemented with complete protease inhibitor cocktail tablet (Sigma, Roche, cat. no. 11697498) according to manufacturer's instructions. Samples (10  $\mu$ g) were separated on Any-kDa Stain-Free SDS-PAGE gels (Criterion TGX, BioRad, cat. no. 5678125), UV activated for detection of total protein levels and blotted onto low fluorescence polyvinylidene fluoride membranes (BioRad, cat. no. 1620263). Membranes were blocked with 5% skim milk in PBS with 0.1% Tween-20. Respective regions were cut from the membranes and incubated over night with primary antibodies directed against HSP60 (Thermo Scientific, cat. no. MA3-013) or HSP10 (Abnova, cat. no. PAB15431). After washing of the membranes with PBS/Tween-20, membranes were incubated for 1 h with the appropriate HRP-conjugated secondary antibodies (goat anti-mouse, Dako cat. no. P0447; goat anti-rabbit, Dako cat. no. P0448; for HSP60 IP: rat anti-mouse TrueBlot® ULTRA, Rockland cat. no. 18-8817-30) and detected with ECL Plus Western Blotting Substrate (Thermo Scientific, cat. no. 32132) using the LAS4000 imaging system (GE Healthcare). Images were analyzed with ImageQuantTL 7.0 software (GE Healthcare).

### Mass spectrometry analysis

For preparation of samples for mass spectrometry (MS) analysis, Filter Aided Sample Preparation (FASP; (Wisniewski et al. 2009)) was used to generate tryptic peptides of the co-immunoprecipitated proteins. In short, samples were diluted threefold in 8 M Urea in 0.1 M Tris pH 8.5 and then concentrated to approximately 15  $\mu$ l in a 10 K filter spin column (Millipore). Proteins were then reduced and alkylated with

10 mM DTT and 50 mM iodoacetamide, respectively, prior to overnight trypsin treatment at 37 °C. The peptide solution was collected by centrifugation followed by peptide fractionation using strong anion exchange (SAX) by stepwise elution from a microcolumn (Rappsilber et al. 2007). Samples were desalted using C-18 purification prior to LC-MS/MS analysis on a nanoAcquity HPLC system coupled to a LTQ-Orbitrap (Thermo) mass spectrometer. Samples were injected onto a home-made 40 cm silica reversed-phase capillary column (New Objective) packed with 3.0  $\mu$ m ReproSil-Pur C18-AQ (Dr. Maisch GmbH). Samples were loaded on the column by the nLC autosampler at a flow rate of 0.5  $\mu$ l per minute. No trap column was used. Peptides were separated by a 150-min gradient of 5–30% between buffer A (0.1% formic acid in water) and buffer B (0.1% formic acid in 80% acetonitrile) at a flow rate of 300 nL/min. MS/MS analysis was performed with standard settings using cycles of one high resolution (70,000 FWHM setting) MS scan followed by MS/MS scans of the 8 most intense ions with charge states of 2 or higher at a resolution setting of 17,500 FWHM.

### Data analysis

Proteins were identified and quantified with MaxQuant software version 1.5.4.1 (Cox and Mann 2008). Default search parameters were used against a human UNIPROT database (version 20190312). Output was sorted in Excel to generate a list of proteins identified and quantified in minimum two out of three experiments.

SCOP protein fold superfamilies were analyzed using the SUPERFAMILY 2 algorithm (<http://supfam.org>, (Gough et al. 2001)). Fold annotations were then extracted from the subordinate superfamily tree level using annotations provided in <http://supfam.org/SUPERFAMILY/function/scop.annotation.1.73.txt>. *P* values were calculated by chi-square analysis (<http://www.statskingdom.com/310GoodnessChi.html>).

## Results and discussion

### Identification of proteins interacting with the HSP60/HSP10 chaperonin

The HSP60/HSP10 chaperonin encapsulates proteins undergoing folding in its central cavity. In order to identify the substrate spectrum of the complex, we performed immunoprecipitation of the HSP60/HSP10 chaperonin from human HEK293 cells followed by mass spectrometric (MS) analysis of the co-immunoprecipitated proteins. We selected a monoclonal anti-HSP60 antibody certified for immunoprecipitation and immunohistochemistry. As an indication for successful immuno-purification of intact chaperonin complexes, we monitored co-immunoprecipitation of HSP10. Western

blotting of the co-immunoprecipitates (co-IPs) only detected co-immunoprecipitated HSP10 protein when cells were treated with the cross-linker DSP (Supplementary Fig. S1A). Furthermore, MS analysis of co-IPs with and without DSP treatment showed significantly increased HSP10 sequence coverage (from approximately 30 to >50%) in samples treated with the cross-linker, indicating clearly higher amounts of co-immunoprecipitated HSP10 protein.

Based on this groundwork, we designed the experimental strategy sketched in Fig. 1. HEK293 cells were grown for at least three cell divisions in medium containing different isotope labeled arginine and lysine (see “Materials and methods”). In each of the three experiments, one batch of cells was exposed to heat stress for 3 h at 43 °C, followed by 12 h recovery at 37 °C before crosslinking and harvesting. We performed the heat shock treatment in order to generate a situation where the mitochondrial protein quality control system is challenged by folding stress. Three hours of heat-shock affected cell morphology and number of attached cells (Supplementary Fig. S1B) and HSP60 levels appeared slightly increased. After 12 h recovery, cell morphology normalized. MS analyses of lysates showed an approximately 15% relative increase of HSP60 protein levels in heat-shocked cells compared with controls. The full experiment was performed in three independent replicates with swapping of SILAC labels between the three samples. Cells were then treated with the cross-linker, harvested, lysed, and subjected to immunoprecipitation using anti-HSP60 or anti-GFP antibodies as indicated in Fig. 1 and described in materials and methods. The anti-GFP antibody was used as a control for unspecific binding to antibodies and beads. The co-IPs from each experiment were mixed, digested with trypsin, and analyzed by nano-LC-MS/MS analysis.

After employing MaxQuant software for identification and quantitation of co-immunoprecipitated proteins, we used the SILAC ratios obtained in the analyses as quantitative measures for the relative amounts of the co-immunoprecipitated proteins. The criteria to be met for classification as an HSP60 interactor were as follows: 1) a SILAC ratio of at least 3 to 1 for the anti-HSP60 immunoprecipitation versus the control anti-GFP antibody and 2) detection in at least two of the three experiments with such a SILAC score. Proteins only detected in the HSP60 co-IP that displayed zero intensity in the GFP co-IP were also judged as fulfilling the SILAC ratio criterion.

Three hundred and twenty-three proteins (313 in the [-HS] and 239 in the [+HS] co-IP inventory) met these criteria (Fig. 2; see full list of proteins in Supplementary Table S1) and were thus defined as HSP60 interactors. Comparison of the list of HSP60 interactors with the

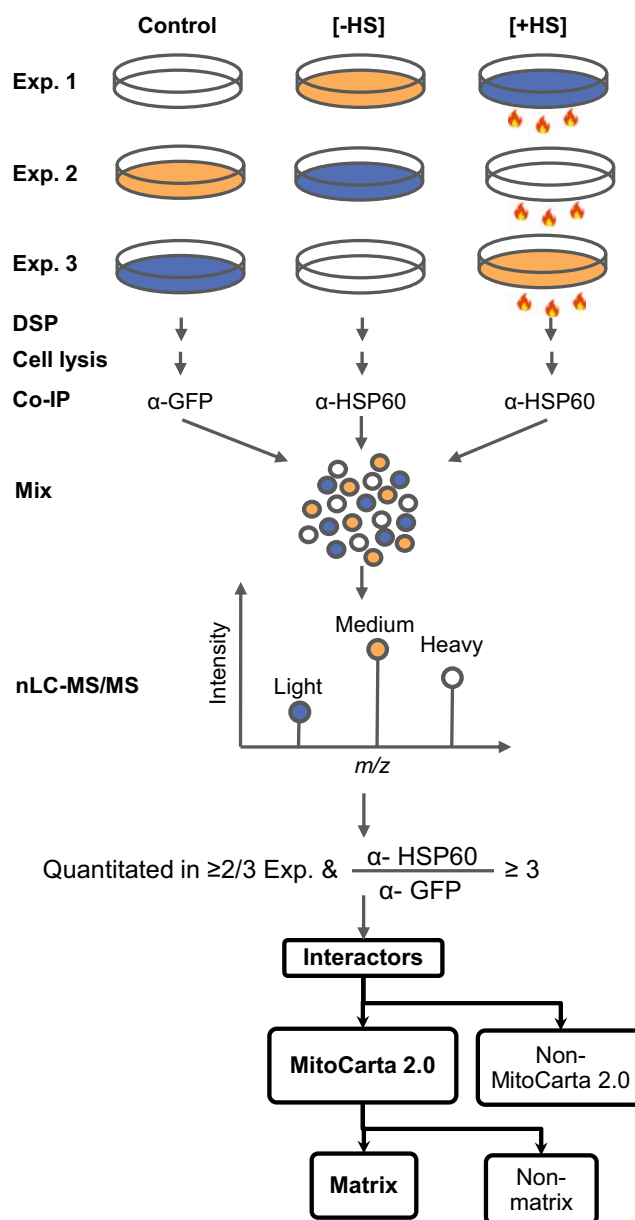
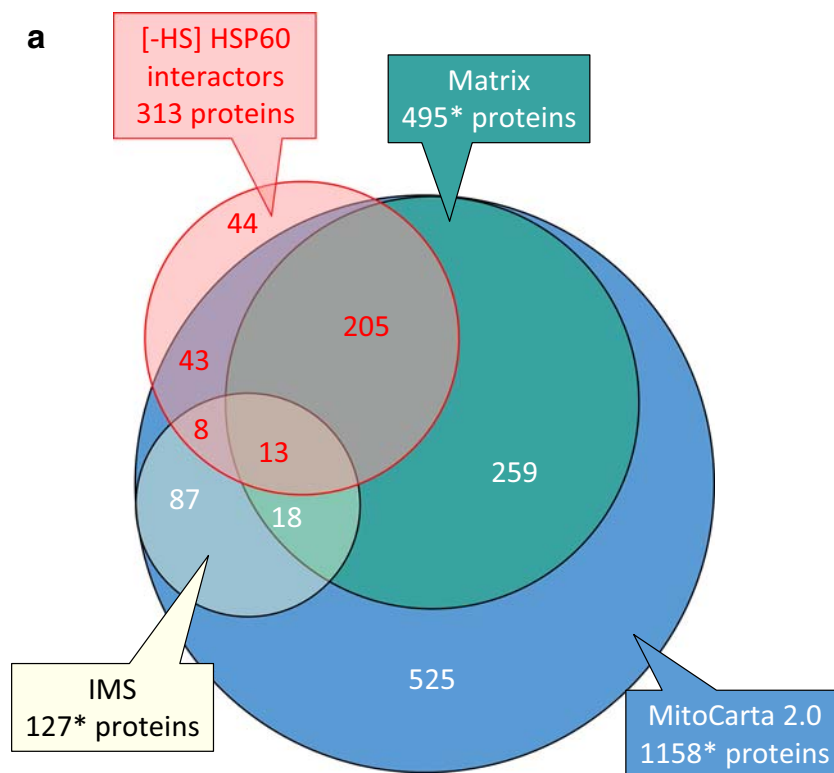


**Fig. 1** Strategy for identification of interactors of the HSP60/HSP10 chaperonin. HEK293 cells were grown at 37 °C in light, medium, and heavy SILAC medium, respectively. One of the cultures in each experiment, [+HS], was treated at 43 °C for 3 h, followed by 12 h of recovery at 37 °C. At the end of incubation, cross-linker was added and cells were subsequently lysed and subjected to immunoprecipitation with antibodies directed against HSP60 ( $\alpha$ -HSP60) or GFP ( $\alpha$ -GFP) as indicated. The three immunoprecipitates were pooled and subjected to nano-LC-MS/MS analysis. The experiment was performed in three independent replicates with swapping of the media as indicated. Proteins quantified in at least 2 of the 3 experiments with a SILAC-ratio  $\geq 3$  between the HSP60 co-IPs versus the GFP co-IP in the respective experiments were classified as HSP60/HSP10 chaperonin interactors. Proteins quantitated in the HSP60 co-IP and having zero intensity in the GFP co-IP were also judged as fulfilling the SILAC ratio criterion. The interactors were cross-checked for presence in the MitoCarta 2.0 inventory of mitochondrial proteins, the inventory of mitochondrial matrix proteins, and the inventory of inter-membrane space proteins



**Fig. 2** Overview of the interactors found. **a** Venn diagram showing the interactors of the HSP60/HSP10 chaperonin identified in the [-HS] co-IPs and assignment to the MitoCarta 2.0 (Calvo et al. 2016), mitochondrial matrix space (Rhee et al. 2013), and mitochondrial intermembrane space (IMS) inventories (Hung et al. 2014). (\*) denotes that the protein numbers do not add up to the total number of proteins in the inventories because HSP60 (part of MitoCarta 2.0, and the matrix inventory) and HSP10 (part of all 3 inventories) are not included. **b** Table giving an overview over protein numbers in the mitochondrial protein inventories and the HSP60 interactors. The numbers of all interacting proteins found, proteins in the [-HS] and [+HS] co-IPs, respectively, and proteins common in both co-IPs are given



MitoCarta 2.0 inventory of mitochondrial proteins (Calvo et al. 2016) revealed that the bulk of HSP60 interactors (276 of 323) are annotated as mitochondrially localized in MitoCarta 2.0. Only 7 of the 276 MitoCarta 2.0 annotated interactors in the [+HS] co-IP inventory were not part of the [-HS] inventory suggesting that the heat shock treatment does not lead to more interactors, but rather to a reduced number of interactors.

Manual inspection of the UNIPROT (<http://www.uniprot.org>) entries for the 47 proteins (44 in the [-HS] and 28 in the [+HS] inventory) not listed as mitochondrial proteins in MitoCarta 2.0 revealed that 17 are involved in cytosolic protein synthesis (including 13 subunits of cytosolic ribosomes), 9 are extramitochondrial molecular chaperones or other folding facilitators, and 4 are cytoskeleton-related proteins. We assume that these proteins either interacted non-specifically with HSP60 or were immuno-captured as interactors of HSP60 during its synthesis on cytosolic ribosomes or during trafficking to the mitochondria.

### The majority of HSP60 interactors are mitochondrial matrix proteins

As the mitochondrial matrix compartment is the site where the HSP60/HSP10 chaperonin performs its chaperoning function, we expected that most of the interacting proteins were mitochondrial matrix proteins. Comparison of the list of the HSP60 interactors with the list of 495 experimentally mapped matrix proteins (Rhee et al. 2013) revealed that altogether 225 proteins (218 in the [-HS] and 172 in the [+HS] co-IP inventory) were matrix proteins (Fig. 2B). This indicates that almost half (45%) of the proteins included in the matrix inventory interact with the HSP60/HSP10 chaperonin. More than 70% of the matrix interactors are annotated in UNIPROT as possessing a mitochondrial transit peptide indicating that they use the standard import pathway into the matrix space via the TIM23 complex in the inner mitochondrial membrane (Pfanner et al. 2019; Wasilewski et al. 2017).

A small number (13) of the HSP60 interactors are listed as being localized in both the matrix and the intermembrane

space (IMS) (Hung et al. 2014; Rhee et al. 2013). These proteins likely span the inner membrane and possess domains emerging into the matrix space. Three of these proteins (COX4I1, COX7A2L, and MT-CO2) are complex IV subunits, with domains in both the IMS and the matrix space (Ghezzi and Zeviani 2012). MT-CO2 is encoded by mitochondrial DNA. We also found another mitochondrial DNA-encoded protein as interactor, MT-ATP6, a subunit of complex V, which is not enclosed in the matrix and IMS inventories. Most of the 13 mitochondrial DNA encoded respiratory chain subunits are highly hydrophobic with multiple transmembrane domains. They have been shown to be co-translationally inserted into the inner membrane (Ott and Herrmann 2010) and are therefore not prime candidates to interact with the HSP60/HSP10 chaperonin in the matrix. MT-CO2 has only two transmembrane domains and it possesses one long and two short hydrophilic stretches. MT-ATP6 also displays hydrophilic regions (Ott and Herrmann 2010). The presence of hydrophilic domains may explain why these two proteins interact with the HSP60/HSP10 chaperonin.

Among the identified chaperonin interactors were also two of the small set of proteins previously reported to depend on the HSP60/HSP10 chaperonin for folding: UQCRC1, a subunit of complex III, and the matrix superoxide dismutase SOD2. Folding of these proteins was impaired in mice heterozygous for a knock-out allele of the *Hspd1* gene encoding murine HSP60 (Magnoni et al. 2013; Magnoni et al. 2014). A large-scale MS study of the total mitochondrial protein interactome of mouse heart reported a multitude of inter- and intra-molecular crosslinks within and between HSP60 and HSP10 molecules, but only six cross-links of HSP60 or HSP10 peptides to potential client proteins (ATP5A1, CS, MDH2, C21ORF33, PPIF, PRDX5) (Liu et al. 2018). Except for PRDX5, they were all identified as HSP60 interactors in our HSP60 interactome. The HSP60 interactome also contains several orthologs of proteins previously found to interact with yeast HSP60, including malate dehydrogenase (MDH2), mitochondrial HSP70 (HSPA9), aconitase (ACO2), the alpha subunit of isocitrate dehydrogenase (IDH3A), thiosulfate sulfurtransferase (TST), and the Rieske Fe/S protein subunit of complex III (UQCRC1) (Cheng et al. 1989; Dubaquié et al. 1998; Hohfeld and Hartl 1994; Ostermann et al. 1989).

### Broad coverage of functions and pathways in the mitochondrial matrix

The HSP60 interactome comprises a broad spectrum of mitochondrial proteins that function in many metabolic pathways including the major energy production pathways: the respiratory chain, the tricarboxylic acid cycle, and fatty acid oxidation (Supplementary Table S1). The largest functional subgroup among the interactors are 74 proteins involved in

mitochondrial protein synthesis. These proteins have a central role for synthesis of the respiratory chain subunits encoded by the mitochondrial DNA. Over half of them (43) are subunits of mitochondrial ribosomes. Another prominent subgroup of interactors related to mitochondrial protein synthesis are 13 mitochondrial t-RNA ligases. Mutations in the genes encoding mitochondrial t-RNA ligases are prominently associated with diseases of the central nervous system (Sissler et al. 2017) and their impaired folding due to genetic deficiency of the HSP60/HSP10 chaperonin could be related to the neuron-specific phenotypes of the chaperonin disorders.

Among the HSP60 interactors are several other components of the mitochondrial quality control machinery: the matrix localized mitochondrial HSP70 chaperone homolog HSPA9 and its co-factors (DNAJA3 and GRPEL1), the mitochondrial HSP90 chaperone homolog TRAP1, the CLPP and CLPX subunits of the matrix CLPXP protease, and the matrix protease LONP1. Besides the possibility that the HSP60/HSP10 chaperonin assists in folding of these proteins, these interactions may also reflect higher order complexes composed of two or more protein quality control components and unfolded or partially folded proteins. Interaction of the matrix protease LONP1 with both HSP60 and HSPA9 has been reported previously in a proteomic study of the LONP1 interactome (Kao et al. 2015).

Another large group of interactors are 33 subunits of respiratory chain complexes including subunits from all five complexes, most of which are exposed to the mitochondrial matrix space (Supplementary Fig. S2).

One hundred and forty five of the genes encoding HSP60 interactors are annotated as disease genes in UNIPROT, including many neurological disease genes. Fifteen of the disease entries mention the term “leukodystrophy,” a phenotype associated with two of the HSP60/HSP10 chaperonin disorders (Bie et al. 2016; Magen et al. 2008). Thirteen of these 15 genes encode subunits or assembly factors of respiratory chain complex I. The two others are PYCR2, associated with a hypomyelinating leukodystrophy, and GLRX5, encoding an iron-sulfur cluster assembly protein.

### Size distribution of HSP60 interactors

Calculations based on the X-ray crystal structure of the *E. coli* GroEL/GroES chaperonin predicted that proteins up to approximately 70 kDa can be accommodated in the closed chaperonin cavity (Xu et al. 1997) and an experimental analysis estimated the maximum size that can be encapsulated to be around 57 kDa (Sakikawa et al. 1999). Among the interactors of *E. coli* GroEL/GroES, proteins with molecular masses between 30 and 50 kDa were overrepresented in relation to the size distribution of all *E. coli* proteins (Kerner et al. 2005). To assess whether the same is the case for the human HSP60 interactors, we plotted the size

distribution profile of the matrix annotated interactors in the [−HS] co-IP (Fig. 3). This showed a pattern similar to the profile for all proteins of the matrix inventory. Proteins with masses between 45 and 60 kDa were slightly overrepresented and proteins with masses below 25 kDa were underrepresented among the HSP60 interactors. The latter is consistent with the notion that small proteins often possess only one domain and fold spontaneously whereas larger multidomain proteins typically require longer time and chaperone interaction for folding and domain arrangement.

A narrow segment of proteins with masses between 100 and 105 kDa were underrepresented; however, 27 matrix proteins with a size larger than 75 kDa were found as interactors of HSP60. One of them is aconitase (ACO2) with a molecular mass of 85.4 kDa. This is in agreement with the finding that the two yeast aconitase homologs, ACO1 and ACO2, have been shown to interact with yeast HSP60 (Dubaque et al. 1998) and in vitro experiments that indicated that GroEL/GroES can assist the folding of yeast aconitase by a binding and release mechanism not involving encapsulation (Chaudhuri et al. 2001).

We also determined the fraction of the total HSP60 capacity that is occupied by proteins in the different size groups. To do this, the matrix-annotated interactors were quantified based on their intensity based absolute quantification (iBAQ) values in the [−HS] co-IPs. The iBAQ value is calculated by summing up the peak intensities of all peptides matching to a specific protein and dividing it by the number of theoretically observable peptides for the respective protein. It is an approximate measure for absolute protein copy numbers, as it corrects for protein size. The sum of iBAQ values in the respective size groups was plotted as percentage fraction of the sum of the iBAQ values of all matrix-annotated [−HS] co-IP

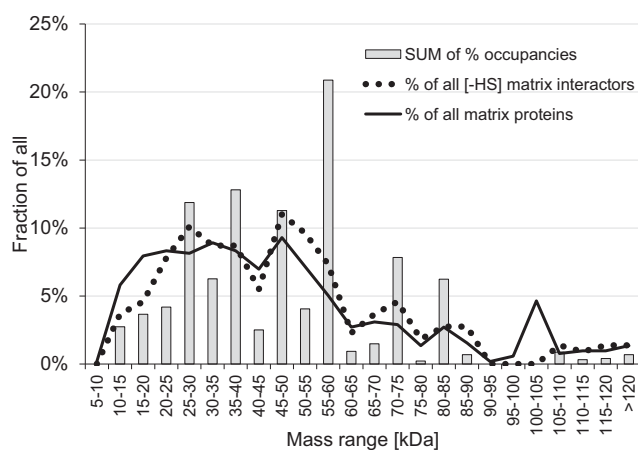


**Fig. 3** Molecular mass distribution of matrix interactors. Comparison of the mass range distributions (percentage of proteins) of the inventory of mitochondrial matrix proteins (black line) (Rhee et al. 2013), with the matrix proteins detected in the [−HS] co-IPs (stippled line). The gray columns give the sum of percent iBAQ for the matrix proteins in the [−HS] co-IP in the respective mass ranges

interactors (columns in Fig. 3). This analysis showed that proteins up to 60 kDa in size occupy ~85% of the total Hsp60 capacity, consistent with the vast majority of interactors being of a size appropriate for encapsulation. There is an overrepresentation of proteins in the mass range 55–60 kDa; however, this is mainly due to the interaction of only 3 proteins with HSP60, 2 subunits of complex V (ATP5A1 and ATP5B), and a serine methylase (SHMT2), which in sum account for almost 20% occupancy.

Classification of the interactors of *E. coli* GroEL according to protein fold type revealed a significant enrichment in the  $(\beta\alpha)_8$  TIM-barrel fold (SCOP class c.1) (Kerner et al. 2005). To test whether certain fold types were enriched in the HSP60 interactome, we compared the fold frequencies in the mitochondrial matrix [−HS] HSP60 interactors to those in the mitochondrial matrix proteome. This analysis revealed no significant over- or underrepresentation of fold types in the HSP60 interactome (Supplementary Fig. S3) The lowest *P* value (chi-square analysis) was 0.1 for the c.66 fold class. The c.1 fold class enriched in GroEL/GroES interactors was slightly but non-significantly underrepresented. It should, however, be noted that the matrix protein inventory only contains 9 SCOP c.1 class proteins which makes it difficult to judge enrichment or diminishment.

### Are certain HSP60 interactors enriched?

In case of the interactors of *E. coli* GroEL, it was possible to distinguish between groups of proteins with different levels of dependence on the chaperonin for folding (Kerner et al. 2005). This was based on the rationale that obligately dependent proteins are most enriched on GroEL, as the whole population of molecules transits through the chaperonin system for folding. Their relative abundance in the chaperonin is therefore greater than their relative cellular abundance. To assess whether we could in a similar way assign the HSP60 interactors into subgroups, we plotted the  $\log_{10}$  iBAQ values for all matrix-annotated interactors in the [−HS] co-IPs versus the cellular abundance of these proteins ( $\log_{10}$  iBAQ) in HEK293 cells. Figure 4 shows the plot of these values. For cellular abundance, we used iBAQ data from a deep proteomic study of the proteomes of 11 human cell lines, including HEK293 cells, by Geiger et al. (Geiger et al. 2012), which covers quantitative values for all HSP60 interactors. If all proteins interact with HSP60 to the same extent, there would be a linear relationship between the abundance in the IP and the abundance in the cell. The plot roughly shows such a relationship as indicated with the regression line. Pearson's correlation analysis showed a positive relationship with a correlation coefficient of 0.558. Proteins identified in both the [−HS] and the [+HS] co-IPs are marked with black circles and proteins only identified in the [−HS] co-IP and not in the [+HS] co-IP are marked with gray squares. The proteins only identified in the

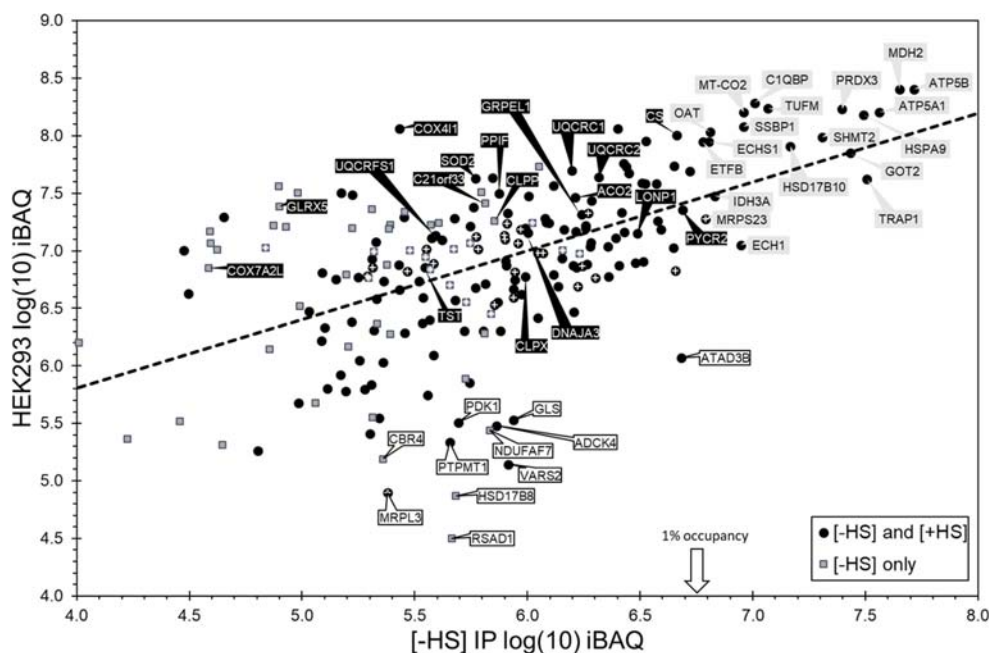


**Fig. 4** Comparison of abundance of HSP60/HSP10 chaperonin interactors with cellular abundance. The log (10) iBAQ values of matrix assigned HSP60/HSP10 chaperonin interactors in the [-HS] co-IPs are plotted against their log (10) iBAQ values in HEK293 cell lysates (Geiger et al. 2012). The values for matrix proteins only identified in the [-HS] co-IP and not in the [+HS] co-IPs are depicted with gray squares and proteins identified in both the [+HS] and the [-HS] co-IPs are depicted with filled black circles. Squares and circles representing ribosomal subunits are marked with white crosses. Linear regression of all data points is shown by the stippled black line. Pearson's correlation analysis showed a

positive relationship with a correlation coefficient of 0.558. The log (10) iBAQ value corresponding to 1% occupancy of the HSP60/HSP10 chaperonin is indicated with an arrow on the horizontal axis. Points for the following subgroups of proteins and proteins referred to in the text are labeled as follows: the 19 proteins accounting for 63% of occupancy (black label on gray background); proteins with relatively high chaperonin occupancy in relation to their cellular abundance (boxed labels); additional proteins mentioned in the text (white label on black background)

[-HS] co-IPs typically display low log (10) iBAQs values on HSP60; in sum less than 3.5% of HSP60/HSP10 occupancy. This may suggest that proteins with low dependence on the chaperonin are supplanted by proteins with higher dependence upon heat shock and recovery treatment.

In contrast, proteins identified in both the [-HS] and [+HS] co-IPs typically displayed high occupancy values. Nineteen proteins (labeled as black text on gray background in Fig. 4) with occupancy values > 1% account for approximately 60% of HSP60/HSP10 chaperonin occupancy. These proteins display also high abundance in HEK293 cells. MDH2, mitochondrial malate dehydrogenase, is a bona fide chaperonin substrate and has extensively been used for measuring in vitro refolding activity of both the GroEL/GroES and the human HSP60/HSP10 chaperonin (Nielsen et al. 1999). HSPA9 and TRAP1 are two matrix protein quality control chaperones that may interact functionally with HSP60.

A group of 11 proteins show markedly higher abundance in the [-HS] co-IP compared with their cellular abundance (ratio of log (10) iBAQ in [-HS] co-IP versus HEK293 total lysate log (10) iBAQ > 1.0; see Supplementary Table S1). This suggests that these proteins display a high dependence on the HSP60/HSP10 chaperonin for folding and conformational maintenance and they may thus be of special interest for

further studies. One of them, the t-RNA ligase VARS2, is associated with several forms of mitochondrial encephalopathies or cardiomyoencephalopathies (Diodato et al. 2014; Taylor et al. 2014).

With the exception of MRPL3, the ribosomal subunits (labeled with white crosses in Fig. 4) display comparable abundances in HEK293 cells (less than tenfold range), while their abundance in the HSP60/HSP10 chaperonin spans over two orders of magnitude. This indicates that the ribosomal subunits are not associated as whole units via bound emerging mitochondrial translation products, but rather interact as single unassembled units.

## Conclusions

Approximately half of the mitochondrial matrix-annotated proteins interact with the HSP60/HSP10 chaperonin. The strong correlation between cellular abundance of these proteins and their occupancy of the HSP60/HSP10 chaperonin suggests a general role of the HSP60/HSP10 chaperonin in the folding of mitochondrial matrix proteins. Just 19 of the interactors account for more than 60% of the mass of the co-



immunoprecipitated proteins; these proteins display also a high cellular abundance.

The high number of mitochondrial matrix proteins interacting with the HSP60/HSP10 chaperonin suggests that the neuronal disorders caused by mutations in the genes encoding the chaperonin subunits or triggered by secondary HSP60/HSP10 chaperonin deficiency are due to impaired folding of a larger group of mitochondrial matrix proteins. Indeed, many of the genes encoding interactors of the HSP60/HSP10 chaperonin interactors are annotated as neurological disease genes. The sum of functional deficiencies in several or many of these proteins due to their impaired folding may cause the disorders. Our inventory of the HSP60 interactome can form the basis for further studies into exploring the dependence of the interactors on the HSP60/HSP10 chaperonin for folding and their contribution to the various disease phenotypes.

**Author contributions** Anne Bie, Peter Bross, Ulrich Hartl, Roman Körner, Thomas Corydon, Johan Palmfeldt, and Mark Hipp contributed to the study conception and design. Data collection and analysis were performed by Anne Bie, Roman Körner, Johan Palmfeldt, Mark Hipp, Cagla Cömert, and Peter Bross. The first draft of the manuscript was written by Anne Bie and Peter Bross. All authors commented on previous versions of the manuscript, and all authors read and approved the final manuscript. Ulrich Hartl and Peter Bross provided resources and lab-facilities.

**Funding information** We thank the HEALTH graduate school, Aarhus University for support (PhD scholarship and travel and material support to A.B.), and the Hede Niensens Fond, and the Deutscher Akademischer Austauschdienst (DAAD) for funding of materials, travel and accommodation.

## References

- Bie AS et al (2016) Effects of a mutation in the HSPE1 gene encoding the mitochondrial co-chaperonin HSP10 and its potential association with a neurological and developmental disorder. *Front Mol Biosci* 3:65. <https://doi.org/10.3389/fmolb.2016.00065>
- Bross P (2015) The Hsp60 Chaperonin. Springer Briefs in Molecular Science. Springer International Publishing, Cham, Switzerland. <https://doi.org/10.1007/978-3-319-26088-4>
- Bross P et al (2008) The Hsp60-(p.V98I) mutation associated with hereditary spastic paraplegia SPG13 compromises chaperonin function both in vitro and in vivo. *JBiolChem* 283:15694. <https://doi.org/10.1074/jbc.M800548200>
- Calvo SE, Clauser KR, Mootha VK (2016) MitoCarta2.0: an updated inventory of mammalian mitochondrial proteins nucleic acids res 44:D1251-D1257. <https://doi.org/10.1093/nar/gkv1003>
- Casari G et al (1998) Spastic paraplegia and OXPHOS impairment caused by mutations in paraplegin, a nuclear-encoded mitochondrial metalloprotease. *Cell* 93:973–983
- Chaudhuri TK, Farr GW, Fenton WA, Rospert S, Horwich AL (2001) GroEL/GroES-mediated folding of a protein too large to be encapsulated. *Cell* 107:235–246
- Cheng MY et al (1989) Mitochondrial heat-shock protein hsp60 is essential for assembly of proteins imported into yeast mitochondria. *Nature* 337:620–625
- Christensen JH et al (2010) Inactivation of the hereditary spastic paraplegia-associated Hspd1 gene encoding the Hsp60 chaperone results in early embryonic lethality in mice. *Cell Stress Chaperones* 15:851–863
- Cox J, Mann M (2008) MaxQuant enables high peptide identification rates, individualized p.p.b.-range mass accuracies and proteome-wide protein quantification. *NatBiotechnol* 26:1367–1372
- Di Bella D et al (2010) Mutations in the mitochondrial protease gene AFG3L2 cause dominant hereditary ataxia SCA28. *Nat Genet* 42:313–321. <https://doi.org/10.1038/ng.544>
- Dikoglu E et al (2015) Mutations in LONP1, a mitochondrial matrix protease, cause CODAS syndrome. *Am J Med Genet A* 167:1501–1509. <https://doi.org/10.1002/ajmg.a.37029>
- Diodato D et al (2014) VARS2 and TARS2 mutations in patients with mitochondrial encephalomyopathies. *Hum Mutat* 35:983–989. <https://doi.org/10.1002/humu.22590>
- Dubaquie Y, Looser R, Fünfschilling U, Jenö P, Rospert S (1998) Identification of in vivo substrates of the yeast mitochondrial chaperonins reveals overlapping but non-identical requirement for hsp60 and hsp10. *EMBO J* 17:5868–5876
- Fayet O, Ziegelhoffer T, Georgopoulos C (1989) The groES and groEL heat shock gene products of *Escherichia coli* are essential for bacterial growth at all temperatures *JBacteriol* 171:1379–1385
- Fujiwara K, Ishihama Y, Nakahigashi K, Soga T, Taguchi H (2010) A systematic survey of in vivo obligate chaperonin-dependent substrates. *EMBO J* 29:1552–1564
- Geiger T, Wehner A, Schaab C, Cox J, Mann M (2012) Comparative proteomic analysis of eleven common cell lines reveals ubiquitous but varying expression of most proteins. *Mol Cell Proteomics* 11: M111. <https://doi.org/10.1074/mcp.M111.014050>
- Ghezzi D, Zeviani M (2012) Assembly factors of human mitochondrial respiratory chain complexes: physiology and pathophysiology. *AdvExpMedBiol* 748:65–106
- Gottesman S, Wickner S, Maurizi MR (1997) Protein quality control: triage by chaperones and proteases. *Genes Dev* 11:815–823. <https://doi.org/10.1101/gad.11.7.815>
- Gough J, Karplus K, Hughey R, Chothia C (2001) Assignment of homology to genome sequences using a library of hidden Markov models that represent all proteins of known structure. *J Mol Biol* 313:903–919. <https://doi.org/10.1006/jmbi.2001.5080>
- Gregersen N, Bross P, Vang S, Christensen JH (2006) Protein misfolding and human disease. *Annu Rev Genomics Hum Genet* 7:103–124. <https://doi.org/10.1146/annurev.genom.7.080505.115737>
- Hansen JJ et al (2002) Hereditary spastic paraplegia SPG13 is associated with a mutation in the gene encoding the mitochondrial chaperonin Hsp60. *Am J Hum Genet* 70:1328–1332
- Hartl FU, Hayer-Hartl M (2009) Converging concepts of protein folding in vitro and in vivo. *Nat Struct Mol Biol* 16:574. <https://doi.org/10.1038/nsmb.1591>
- Hayer-Hartl M, Bracher A, Hartl FU (2016) The GroEL-GroES Chaperonin Machine: A Nano-Cage for Protein Folding *Trends Biochem Sci* 41:62–76. <https://doi.org/10.1016/j.tibs.2015.07.009>
- Hipp MS, Kasturi P, Hartl FU (2019) The proteostasis network and its decline in ageing. *Nat Rev Mol Cell Biol* 20:421–435. <https://doi.org/10.1038/s41580-019-0101-y>
- Hohfeld J, Hartl FU (1994) Role of the chaperonin cofactor Hsp10 in protein folding and sorting in yeast mitochondria. *J Cell Biol* 126:305–315
- Houry WA, Frishman D, Eckerskorn C, Lottspeich F, Hartl FU (1999) Identification of in vivo substrates of the chaperonin. *GroEL Nature* 402:147–154. <https://doi.org/10.1038/45977>

- Hung V et al (2014) Proteomic mapping of the human mitochondrial intermembrane space in live cells via ratiometric APEX tagging. *Mol Cell* 55:332–341. <https://doi.org/10.1016/j.molcel.2014.06.003>
- Jenkinson EM et al (2013) Perrault syndrome is caused by recessive mutations in CLPP, encoding a mitochondrial ATP-dependent chambered protease. *Am J Hum Genet* 92:605–613
- Kao TY et al (2015) Mitochondrial Lon regulates apoptosis through the association with Hsp60-mtHsp70 complex. *Cell Death Dis* 6:e1642. <https://doi.org/10.1038/cddis.2015.9>
- Kerner MJ, Naylor DJ, Ishihama Y, Maier T, Chang HC, Stines AP, Georgopoulos C, Frishman D, Hayer-Hartl M, Mann M, Hartl FU (2005) Proteome-wide analysis of chaperonin-dependent protein folding in *Escherichia coli*. *Cell* 122:209–220
- Kim YE, Hipp MS, Bracher A, Hayer-Hartl M, Hartl FU (2013) Molecular chaperone functions in protein folding and proteostasis. *Annu Rev Biochem* 82:323–355
- Levy-Rimler G, Bell R, Ben Tal N, Azem A (2002) Type I chaperonins: not all are created equal *FEBS Lett* 529:1
- Levy-Rimler G et al. (2001) The effect of nucleotides and mitochondrial chaperonin 10 on the structure and chaperone activity of mitochondrial chaperonin 60 *Eur J Biochem* 268:3465–3472
- Liu F, Lossel P, Rabbitts BM, Balaban RS, Heck AJR (2018) The interactome of intact mitochondria by cross-linking mass spectrometry provides evidence for coexisting respiratory supercomplexes. *Mol Cell Proteomics* 17:216–232. <https://doi.org/10.1074/mcp.RA117.000470>
- Magen D et al (2008) Mitochondrial hsp60 chaperonopathy causes an autosomal-recessive neurodegenerative disorder linked to brain hypomyelination and leukodystrophy. *Am J Hum Genet* 83:30–42
- Magnoni R et al (2013) Late onset motoneuron disorder caused by mitochondrial Hsp60 chaperone deficiency in mice. *Neurobiol Dis* 54:12–23. <https://doi.org/10.1016/j.nbd.2013.02.012>
- Magnoni R, Palmfeldt J, Hansen J, Christensen JH, Corydon TJ, Bross P (2014) The Hsp60 folding machinery is crucial for manganese superoxide dismutase folding and function. *Free Radic Res* 48:168–179. <https://doi.org/10.3109/10715762.2013.858147>
- Nielsen KL, McLennan N, Masters M, Cowan NJ (1999) A single-ring mitochondrial chaperonin (Hsp60-Hsp10) can substitute for GroEL-GroES in vivo. *J Bacteriol* 181:5871–5875
- Nisemblat S, Yaniv O, Parnas A, Frolow F, Azem A (2015) Crystal structure of the human mitochondrial chaperonin symmetrical football complex *Proceedings of the National Academy of Sciences of the United States of America* 112:6044–6049. <https://doi.org/10.1073/pnas.1411718112>
- Ong SE, Mann M (2006) A practical recipe for stable isotope labeling by amino acids in cell culture (SILAC). *Nature Protocols* 1:2650–2660. <https://doi.org/10.1038/nprot.2006.427>
- Ostermann J, Horwich AL, Neupert W, Hartl FU (1989) Protein folding in mitochondria requires complex formation with hsp60 and ATP hydrolysis. *Nature* 341:125–130
- Ott M, Herrmann JM (2010) Co-translational membrane insertion of mitochondrially encoded proteins. *Biochim Biophys Acta* 1803:767–775. <https://doi.org/10.1016/j.bbamcr.2009.11.010>
- Perezgasga L, Segovia L, Zurita M (1999) Molecular characterization of the 5' control region and of two lethal alleles affecting the hsp60 gene in *Drosophila melanogaster* *FEBS Lett* 456:269–273
- Pfanner N, Warscheid B, Wiedemann N (2019) Mitochondrial proteins: from biogenesis to functional networks. *Nat Rev Mol Cell Biol* 20:267–284. <https://doi.org/10.1038/s41580-018-0092-0>
- Rappsilber J, Mann M, Ishihama Y (2007) Protocol for micro-purification, enrichment, pre-fractionation and storage of peptides for proteomics using StageTips. *Nat Protoc* 2:1896. <https://doi.org/10.1038/nprot.2007.261>
- Rhee HW, Zou P, Udeshi ND, Martell JD, Mootha VK, Carr SA, Ting AY (2013) Proteomic mapping of mitochondria in living cells via spatially restricted enzymatic tagging. *Science (New York, NY)* 339:1328–1331
- Royer-Bertrand B et al (2015) Mutations in the heat-shock protein A9 (HSPA9) gene cause the EVEN-PLUS syndrome of congenital malformations and skeletal dysplasia. *Sci Rep* 5:17154. <https://doi.org/10.1038/srep17154>
- Saijo T, Welch WJ, Tanaka K (1994) Intramitochondrial folding and assembly of medium-chain acyl-CoA dehydrogenase (MCAD) - demonstration of impaired transfer of K304E-variant MCAD from its complex with Hsp60 to the native tetramer. *JBiolChem* 269:4401–4408
- Saisawat P et al (2014) Whole-exome resequencing reveals recessive mutations in TRAP1 in individuals with CAKUT and VACTERL association. *Kidney Int* 85:1310–1317. <https://doi.org/10.1038/ki.2013.417>
- Sakikawa C, Taguchi H, Makino Y, Yoshida M (1999) On the maximum size of proteins to stay and fold in the cavity of GroEL underneath GroES. *J Biol Chem* 274:21251–21256
- Sissler M, Gonzalez-Serrano LE, Westhof E (2017) Recent advances in mitochondrial aminoacyl-tRNA synthetases and disease. *Trends Mol Med* 23:693–708. <https://doi.org/10.1016/j.molmed.2017.06.002>
- Szegő ÉM et al (2019) Cytosolic trapping of a mitochondrial heat shock protein is an early pathological event in synucleinopathies. *Cell Rep* 28:65–77.e66. <https://doi.org/10.1016/j.celrep.2019.06.009>
- Taylor RW et al (2014) Use of whole-exome sequencing to determine the genetic basis of multiple mitochondrial respiratory chain complex deficiencies. *Jama* 312:68–77. <https://doi.org/10.1001/jama.2014.7184>
- Wasilewski M, Chojnacka K, Chacinska A (2017) Protein trafficking at the crossroads to mitochondria. *Biochim Biophys Acta* 1864:125–137. <https://doi.org/10.1016/j.bbamcr.2016.10.019>
- Wisniewski JR, Zougman A, Nagaraj N, Mann M (2009) Universal sample preparation method for proteome analysis. *Nat Methods* 6:359–362. <https://doi.org/10.1038/nmeth.1322>
- Xu ZH, Horwich AL, Sigler PB (1997) The crystal structure of the asymmetric GroEL-GroES- (ADP)(7) chaperonin complex. *Nature* 388:741–750

**Publisher's note** Springer Nature remains neutral with regard to jurisdictional claims in published maps and institutional affiliations.